FIFTH INTERNATIONAL CONGRESS ON SOUND AND VIBRATION
DECEMBER 15-18, 1997
ADELAIDE, SOUTH AUSTRALIA

Specialist Keynote Paper

SOME RECENT ADVANCES IN SIGNAL PROCESSING FOR VIBRATION MONITORING

Joseph Mathew
Chair in Manufacturing and Industrial Engineering
Department of Mechanical Engineering
Monash University
P O Box 197, Caulfield East, Victoria 3145

ABSTRACT

Vibration condition monitoring is now a well accepted part of an effective plant-wide condition monitoring program. Several techniques have been developed in recent years to assist vibration engineers detect and diagnose faults in machinery (Mathew 1987). This paper is concerned with two of these newer techniques, viz, the application of chaos theory and neural networks to vibration monitoring. The article is presented in two parts; Part I is concerned with chaos theory and Part II describes an application of neural networks to rolling element bearing fault diagnosis.

PART 1 - CHAOS THEORY (co-authored by Mr David Logan)

1 NOMENCLATURE

$C(l)$	:	correlation integral;
d_G	:	correlation dimension;
k	:	offset preventing vectors spatially close being counted, leading to possibly spurious correlations;
K	:	Kolmogorov, or information, entropy;
l	:	hypersphere[1] radius inside which points are counted;
m	:	embedding phase space dimension;
p	:	spacing between first element of each reconstructed vector;
M	:	number of vectors reconstructed from original time series;
$\tilde{X}_i$	:	position vector (in m dimensions) of point on phase space attractor;
r^2	:	line fit 'quality' coefficient;
τ	:	spacing between points within each reconstructed vector;
$\Theta(x)$	:	Heaviside step function, unity if $x > 0$, zero if $x \leq 0$.

[1] A hypersphere is a sphere of arbitrary dimension. A two dimensional hypersphere is a circle, a three dimensional one, a conventional sphere.

2 INTRODUCTION

Despite the wide proliferation of condition monitoring techniques currently in use, there has yet been very little attention paid to the occurrence or importance of chaotic behaviour as an indicator of the condition of rotating machinery. Extensive descriptions of the basic principles of chaos can be found in Crutchfield et al. (1986), Baker and Gollub (1990) or Logan et al. (1992), but a common misconception about chaos should first be clarified. Chaotic behaviour is not synonymous with stochastic (random) behaviour. Irregularity in a random system results from unpredictable outside influences, while the variability in a chaotic system is inherent - it is a function of the system's intrinsic dynamic characteristics. Chaotic systems are deterministic, but the exponential propagation of errors means that predictions are only possible for short periods. The motion of a dynamical system can be best represented by transforming it onto its phase space. The phase space of a system has been defined in Baker and Gollub (1990) as '... a mathematical space with orthogonal co-ordinate directions representing each of the variables needed to specify the system.' The phase space of a simple pendulum, for example, would be two dimensional with axes of position and velocity (θ and ω). Each of the instantaneous states of a system can be plotted on its phase space, after transient effects have decayed. The complete set of these points encompasses every location in phase space that is 'visited' by the system, and is known as its attractor. The geometric form of an attractor, related to its chaoticity, can be quantified by measuring its dimension. This study investigates the application of one particular fractal dimension, the correlation dimension (d_G), to a vibration acceleration time series collected from a simple rolling element bearing test rig. Bearings in both new and faulty states have been tested and the relationship between d_G and bearing fault investigated.

3 CALCULATING FRACTAL DIMENSION

3.1 EMBEDDING THE TIME SERIES

To measure the fractal dimension of an arbitrary time series, such as that collected from vibration acceleration data, the attractor must first be reconstructed, then its dimension computed. For a system where the differential equations of motion are known, this procedure is relatively simple, since the characteristic variables of the system are known. For more complex systems, that may be difficult or impossible to model accurately, the characteristic variables may not be known. The only option for reconstructing the attractor is then to use the time delay technique. This is described in several references, including Froehling et al. (1981), Grassberger and Procaccia (1983b and 1983c) and Simm et al. (1987). Briefly, it involves selecting time series elements at pre-determined intervals and using these to represent points in phase space. Instead of the phase space axes being θ and ω, for example, they will be t and $t+\Delta t$ for a two dimensional phase space, t, $t+\Delta t$ and $t+2\Delta t$ for three dimensions, and so on according to the dimension of the phase space desired for embedding the attractor.

Take a time series, $\tilde{X}_i$, consisting of N elements, each separated by time delay, Δt.

$$\left\{\tilde{X}_i = X(k\Delta t)\right\}_{i=1}^{N} \tag{1}$$

From this time series, a set of m-dimensional vectors is constructed:

$$\begin{aligned}
\tilde{x}_1 &= \{x_1, x_{\tau+1}, x_{2\tau+1}, \cdots, x_{(m-1)\tau+1}\} \\
\tilde{x}_2 &= \{x_{p+1}, x_{p+\tau+1}, x_{p+2\tau+1}, \cdots, x_{p+(m-1)\tau+1}\} \\
&\vdots \\
\tilde{x}_M &= \{x_{Mp+1}, x_{Mp+\tau+1}, x_{Mp+2\tau+1}, \cdots, x_{Mp+(m-1)\tau+1}
\end{aligned} \tag{2}$$

Selection of the appropriate parameters is a different exercise and involves both guidelines given in Simm et al. (1987) and an analysis of the relationships between d_G and the various parameters to determine their ranges of stability.

3.2 COMPUTING THE CORRELATION INTEGRAL

Now that the attractor has been reconstructed, the remaining task is to compute the dimension of the attractor. There are several types of dimensions, but the correlation dimension has been found to be accurate and computationally efficient for large dimensional attractors (Greenside et al., 1982). The correlation dimension is derived from the correlation integral:

$$C(l) = \lim_{M\to\infty}\left[\frac{2}{M^2}\sum_{i=1}^{M-k}\sum_{j=i+k}^{M}\Theta\left(l - \left|\tilde{X}_i - \tilde{X}_j\right|\right)\right] \tag{3}$$

The terms used in this equation are all defined in Section 1, Nomenclature. The Heaviside step function, $\Theta\left(l - \left|\tilde{X}_i - \tilde{X}_j\right|\right)$, simply counts the number of reconstructed vectors closer than distance, l, to one another, while $C(l)$ yields the average fraction of points within distance, l.

To calculate the correlation dimension, d_G, a range of values for l is chosen and the correlation integral calculated for each. A log-log plot of $C(l)$ versus l is then plotted and the slope of the central, straight line portion of the graph yields d_G. The graph takes on a sigmoidal shape, as in Figure 1.

This shape results from the characteristics of the correlation integral. The minimum number of

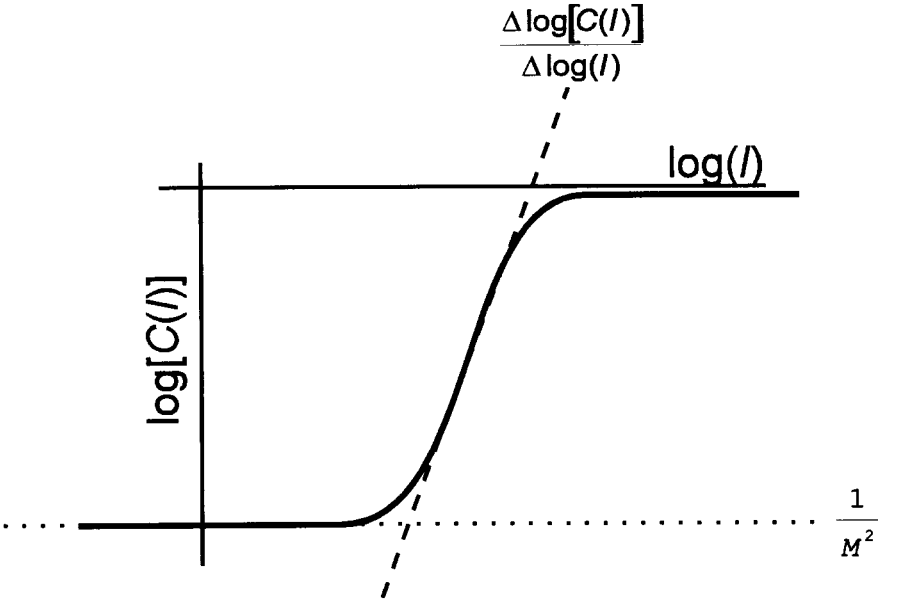

Figure 1. Ideal correlation integral plot

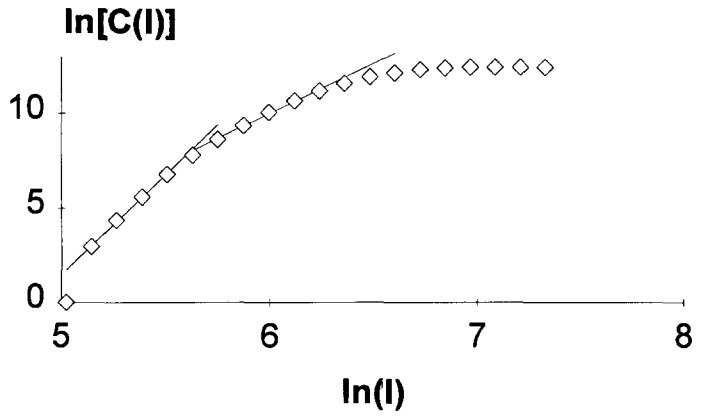

Figure 2. Practical correlation integral plot

vectors that can be counted is one (the vector itself) and hence the integral asymptotes to $1/M^2$. The maximum number of vectors saturates at M, since a hypersphere of large enough radius will encompass all points on the attractor. The slope of the straight line region in the centre of the graph yields the dimension of the reconstructed attractor.

In practice, the process is not quite so straightforward. When actual time series data is analysed, a certain level of noise is superimposed on the data. Noise appears as a steeper slope towards the left side of the graph, breaking downwards to a shallower, chaotic slope on the right side of the plot (Figure 2). The two slope behaviour can be seen clearly in this figure.

3.3 ATTRACTOR EMBEDDING AND CORRELATION INTEGRAL PARAMETERS

The selection process for obtaining the optimum parameters for determining the correlation integral is beyond the scope of this study, but Simm et al. (1987) is useful. A total of 3000 points was used to embed the time series and a dimension of 15 for the phase space.

4 EXPERIMENTAL EQUIPMENT

The test rig consisted of a single double row rolling element bearing mounted on a shaft between two taper roller support bearings, which were designed to fail over a much longer period than the test bearing. Details of the test bearing are given in Table 1.

The shaft upon which the bearing was mounted was driven at a constant speed of 3000 rpm (50 Hz) by a three phase electric motor driving through a flexible coupling. A constant load force, F, was provided by a hydraulic jack.

A TEAC DAT recorder was used to store the raw data collected from the rig in order to effectively test different sampling rates and data algorithms without the need to retest bearings. A minimum amount of preprocessing of the data was performed, with the system consisting solely of a piezo-electric accelerometer and a charge amplifier. The reason for this is that Möller et al. (1989) suggests that distortion of chaotic behaviour occurs through the addition of noise from components such as filters and rectifiers.

Table 1. Test bearing details

Parameter		***value***
Model		SKF 2209
Shaft diameter	(mm)	45.0
Pitch circle diameter	(mm)	64.0
Rolling element diameter	(mm)	11.5
Number of rolling elements		30 (15 x 2 rows)
Rotational frequency	(Hz)	50
Outer race defect frequency	(Hz)	308
Inner race defect frequency	(Hz)	443
Roller fault frequency	(Hz)	21

An RTI 860 model analogue-digital card was used to digitise the raw data, with 12 bit resolution. The values available from the card were thus integers ranging from -2048 to 2047, with a theoretical resolution of one part in 4096. A bandwidth of 2 kHz was imposed upon the data for this testing program (approximately four harmonics of the inner race fault frequency), using a sampling rate of 4 kHz to prevent aliasing.

5 TESTING PROGRAM

Four bearings, nominally identical, were used in the testing program. Three bearing faults were induced and compared with the normal bearing as a control case. Details of the bearings tested are as follows:

1. "Normal": A new bearing was run in at light load for around six hours before data was collected.
2. "Outer": A severe outer race fault, approximately 1.5 mm in width was electric arc inscribed across the outer race perpendicular to the ball path of a new bearing.
3. "Inner": An inner race fault, similar in form and size to the outer race fault above, was generated on the inner race of a new bearing.
4. "Roller": A single rolling element was removed from the race, roughened by sand-blasting and reinstalled in the bearing.

A custom program was written to compute the correlation dimension, since no software currently exists to perform this task. It was programmed in Turbo Pascal and entitled 'Correl' (rhyming with 'coral'). It is partly event-driven and has fully modular design. Over 3000 lines of code perform the following functions:

(a) Generate phase space vectors from ASCII file of integer or floating point raw time series data.
(b) Compute the correlation integral for an appropriate range of hypersphere radii.
(c) Output results to ASCII format file for analysis in other packages, such as spreadsheets.
(d) Plot results to allow straight line of best fit to be overlayed and d_G to be calculated.

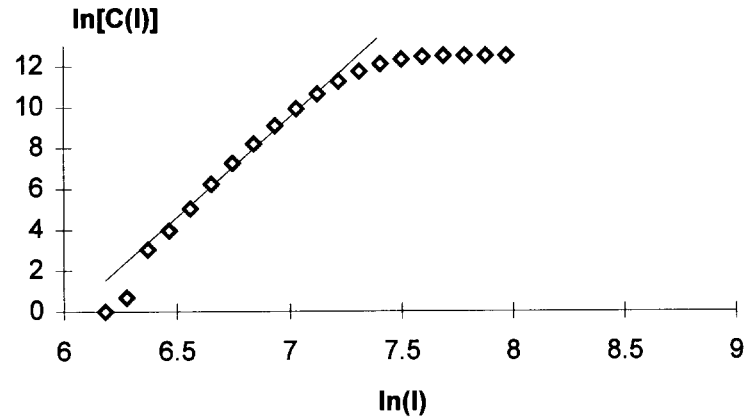

Figure 3. Typical correlation integral plot for "Normal" bearing. Mean: 11.0, Standard deviation: 0.9 (8%)

Unfortunately, selecting the appropriate portion of the correlation integral plot has to be carried out manually, since an algorithm has not been devised to identify this region automatically. The line of best fit is computed using a least squares' regression analysis of the data (Kreysig, 1988), with the appropriate points being interactively included or excluded from the plot by the user.

6 TEST RESULTS

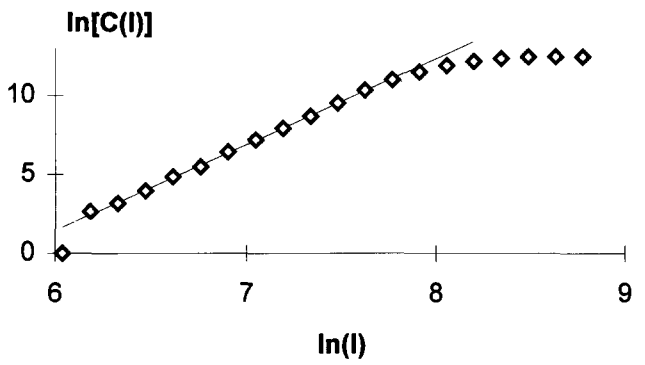

Figure 4. Typical "Outer" bearing.
Mean: 5.4, Standard deviation: 0.3 (6%)

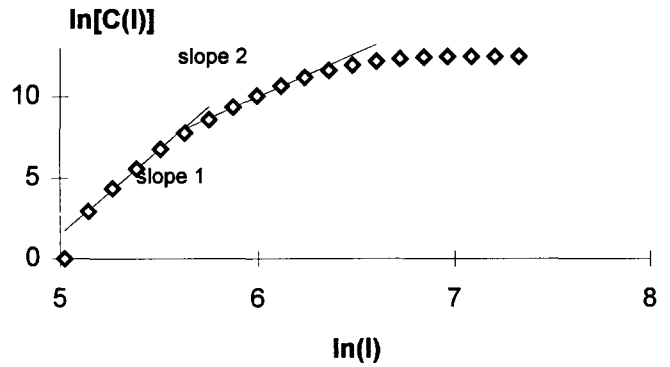

Figure 5. Typical "Inner" bearing plot.
Mean: 10.2, 6.3, Standard deviation: 1.8, 0.8 (18%, 13%)

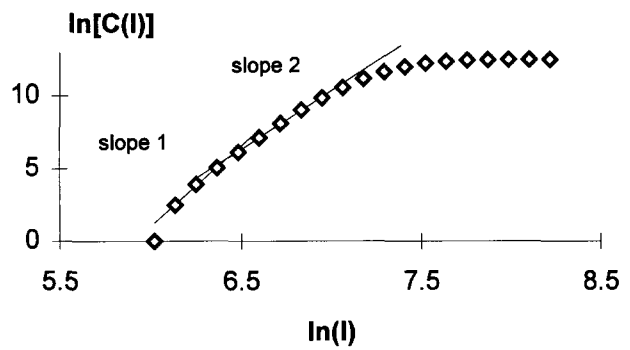

Figure 4. Typical "Roller" bearing plot.
Mean: 10.5, 7.4, Standard deviation: 1.8, 0.5 (17%, 7%)

In each of the following sub-sections, the table lists the mean values obtained for the data samples collected (usually 15 samples). As each sample of 3000 points required less than a second to acquire, the samples were spread out to 10 second intervals to give a representative portion of the collected time series. In addition the standard deviation and the ratio between the standard deviation and the mean, expressed as a percentage, are also given.

The axis scales on the plots in this section are relative and should not be regarded as necessarily representing any absolute values. The relative scales between individual graphs have been maintained constant for comparison.

6.1 "NORMAL" BEARING

The normal bearing exhibited behaviour typical of a time series with mainly random components. The plots were inconsistent in form, some exhibiting steep slopes characteristic of random noise, while others appeared to have shallower slopes indicative of more deterministic behaviour. The overall result averaged to a single slope, as shown in Figure 3.

6.2 "OUTER" BEARING

The "Outer" fault was the most consistent of any of the bearings, with an attractor dimension varying little from an average of $d_G = 5.4$ (Figure 4). Most of the correlation integral plots appeared as in Figure 4.

6.3 "INNER" BEARING

The induced inner race fault correlation integral plots generally had two distinct slopes (see Figure 5), a steep slope resulting from

random noise breaking to a shallower, deterministic slope. Approximately 65% of the samples had a steep slope for the width of the graph, indicating excessive levels of noise obscuring any chaotic behaviour present.

6.4 "ROLLER" BEARING

Forty percent of the "Roller" bearing samples collected displayed a break from higher to a lower dimension. The remainder were dominated by random noise with only a single slope. An example is shown in Figure 6.

7 DISCUSSION ON CHAOS

The correlation dimension certainly distinguishes quite effectively between the normal, undamaged bearing and a faulty one. Figure 7 demonstrates clearly that the range of values expected for faulty bearings will rarely overlap with the range for a normal one. Furthermore, the spread of values for each of the faults is small enough that if sufficient samples are taken from the time series and averaged, as demonstrated within this paper, it is quite feasible to make confident decisions regarding the presence and type of fault in a bearing. Finally, the time required to compute the correlation dimension, for the combination of parameters used, including time series reconstruction, is only around 20 minutes on a fast Intel 486-based machine.

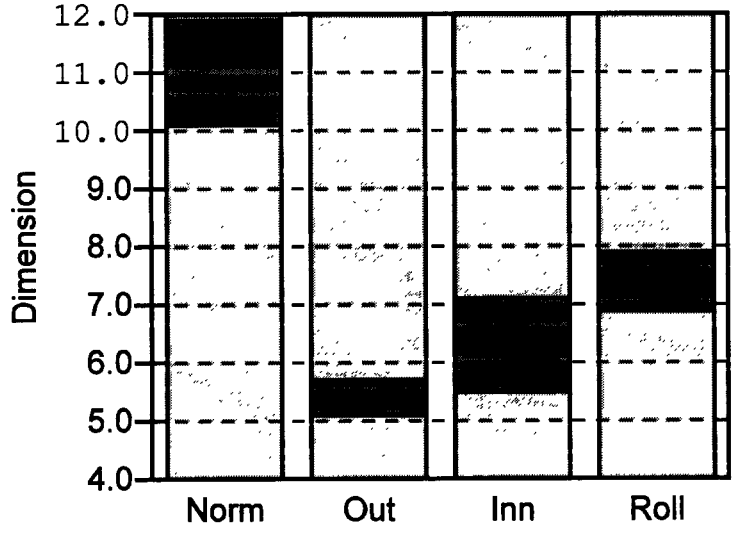

Figure 7. Fractal dimension range versus fault type. The lower and upper extents of the lines represent one standard deviation either side of the mean value (indicated by the horizontal bar)
Norm = "Normal", Out = "Outer", Inn = "Inner", Roll = "Roller

Future work will encompass the problem of deterioration trending: can the correlation dimension be used to identify a fault as it arises in the bearing? This is certainly more important from a practical viewpoint than simply being able to confirm known faults.

PART II – FAULT DIAGNOSIS OF BEARINGS USING SHORT DATA LENGTHS

(co-authored by Mr David Baillie)

8 INTRODUCTION

Fault diagnosis of rolling element bearings have typically been carried out by identifying features in the frequency spectrum of the vibration signal. However, this method of fault classification may not always be appropriate. In situations where only short data lengths are available (such as slow or varying speed machinery), the Fourier Transform is largely unreliable. Techniques of diagnosing faults directly from the time domain vibration signal must be employed. A novel model-based fault diagnostic system based on a set of parametric models of the vibration signal is proposed in this paper. The effect of the vibration data length on the reliability and accuracy of fault classification is investigated for a rolling element bearing.

9 MODEL-BASED FAULT DIAGNOSIS

The model-based fault diagnostic system consists of a number of parametric models that observe the time domain vibration signal emanating from the rotating bearing (Figure 8). Each individual model is built to represent a certain class of fault. The model which best represents the vibration signature is declared to indicate the current state of the machine.

Previous work by Baillie and Mathew (1994) has demonstrated that rolling element bearing vibration signals can be accurately modelled by a general autoregressive process (Box and Jenkins 1976) of the form (Eq 4):

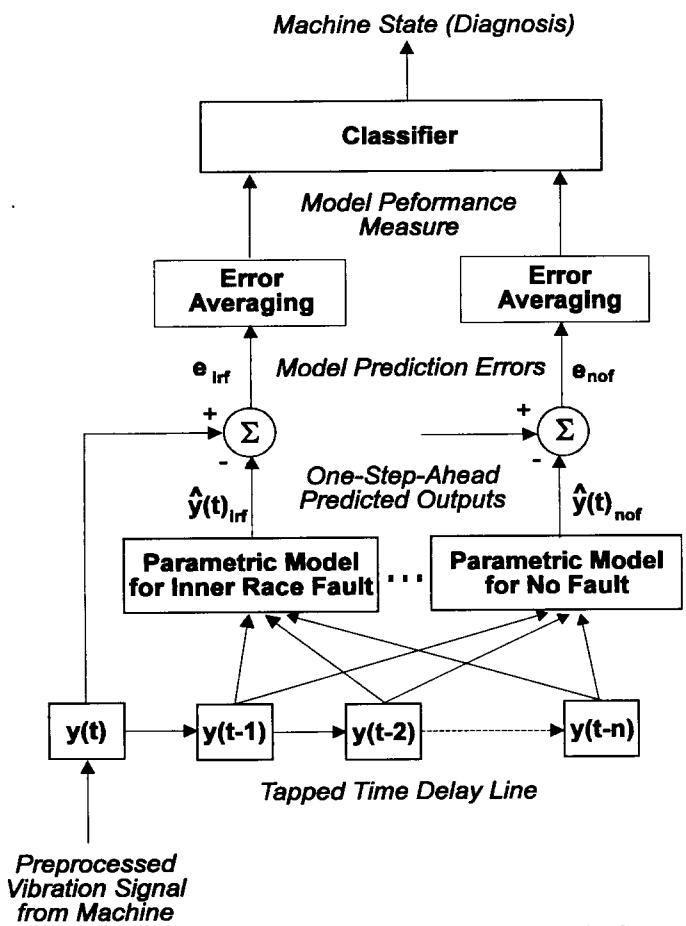

Figure 8. Model-Based Fault Diagnostic System

$$\hat{y}(t) = f\{y(t-1), y(t-2), \ldots, y(t-n)\} \quad (4)$$

where $\hat{y}(t)$ is the "one-step-ahead" predicted model output

y(t-n) are past system vibrations

The autoregressive model effectively provides a "one-step-ahead" prediction of the vibration signal, as the function uses previous outputs regressed on to itself to provide an estimate of the current output. A double-layer Backpropagation neural network provides a convenient method to implement the general autoregressive models, as it is able to successfully learn the complex nonlinear mappings between the input and output signals.

The Backpropagation neural network is based on the

Backpropagation training algorithm popularised by Rumelhart et al (1986). Figure 9 illustrates the general architecture of the neural network. The input layer receives the incoming vibration time series vector from the bearing, and distributes the signal to the hidden layer. The hidden layer is associated with intermediate processing of the signal, while in the output layer, the internal signal is nonlinearly combined to provide the predicted output signal. The mapping performed by the neural network can be expressed by (Eq 5), assuming the processing element transfer functions are nonlinear sigmoids.

$$\hat{y}(t) = \frac{1}{1 + exp\left(-\sum_j w_{kj}.u_j\right)} \tag{5}$$

where,

$$u_j = \frac{1}{1 + exp\left(-\sum_i w_{ji}.y(t-i)\right)}$$ (hidden layer node activations)

w are the neural network internal connection weights.

The accuracy of the autoregressive model is usually determined by the modelling error between the predicted model output and the actual process output (Eq 6).

$$e(t) = y(t) - \hat{y}(t) \tag{6}$$

where $e(t)$ is the model prediction error.

By averaging the model prediction errors over a number of predictions made by the neural network, the statistical fluctuations can be filtered out. The performance of each model can then be gauged from the Signal to Noise Ratio (Eq 7). The Signal to Noise ratio effectively compares the average modelling error to the average power in the vibration signal.

$$SNR = log_{10}\left(\frac{\sum\left(y(t) - \bar{y}(t)\right)^2}{\sum e(t)^2}\right) \tag{7}$$

where SNR is the Signal to Noise Ratio (units of dB)

$\bar{y}(t)$ is the mean of the time series signal

The model-based fault diagnostic system employs a classification stage to interpret the performance of each autoregressive model. Based upon the Signal to Noise ratio of each model, the classifier will determine which class of fault the vibration signal belongs to. This investigation used Baye's rule (Eq 8) to statistically classify the Signal to Noise ratios from each model.

$$P(M_i|SNR_i) = \frac{p(SNR_i|M_i).P(M_i)}{\sum_j p(SNR_i|M_j).P(M_j)} \tag{8}$$

where

- $P(M_i|SNR_i)$ is the Probability of Fault Existence that the Signal to Noise Ratio (SNRi) corresponds to the parametric model of fault type class i (Mi),
- $p(SNR_i|M_i)$ is the conditional probability density function of the Signal to Noise Ratio for a given fault model,
- P(Mj) is the a priori probability of the occurrence of a fault of type j.

10 BEARING FAULT DIAGNOSIS

The data obtained for the series of experiments was from a rolling element test rig designed by the author. The test bearing was a double-row self-aligning type bearing, and was radially loaded at a

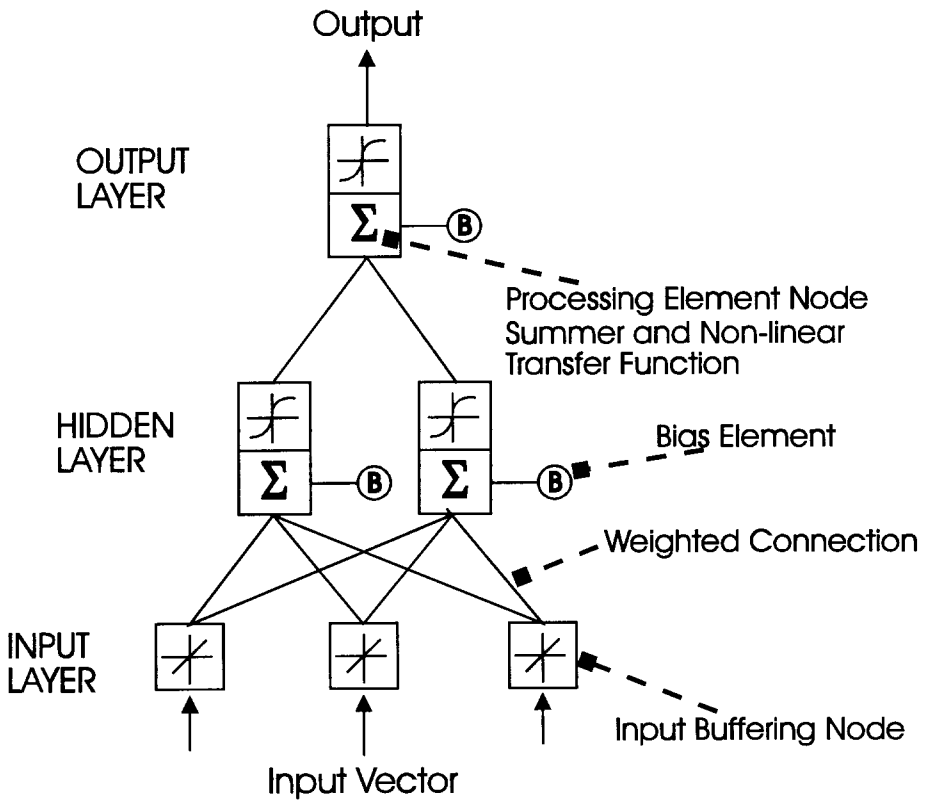

Figure 9. Typical Two-Layer Backpropagation Neural Network

constant force of 9.0 kN. A piezo-electric accelerometer was mounted on the bearing housing, and the shaft was spun at a steady speed of 3000 rpm. The bearing specifications are detailed in Table 2.

Four classes of bearing condition were considered in this investigation:

(a) An artificially induced inner race fault across both raceways (IRF). The fault was etched in the race by electro-discharge machining.

(b) An artificially induced outer race fault across both raceways (ORF). This fault was also initiated by electro-discharge machining of the race.

(c) An artificially induced rolling element fault on two adjacent rolling elements (REF). This fault was simulated by grinding a flattened surface on a ball.

(d) A normal bearing in a serviceable condition (NOF). This was a new bearing after a few hours of running in on the test rig.

Table 2. Test Bearing Specifications

Bearing Specifications	
Bearing Type	SKF 2209E Double Row
Pitch Diameter	64.0 mm
Ball Diameter	11.5 mm
Balls per Row	15
Contact Angle	0 deg
Bearing Load	9.0 kN, Radial Direction
Characteristic Fault Frequencies	
Shaft Speed	50 Hz
Ball Cage Rotation	21 Hz
Ball Rotation	270 Hz
Outer Race Ball Pass	308 Hz
Inner Race Ball Pass	442 Hz

The vibration signal was conditioned by a charge preamplifier prior to envelope detection (amplitude demodulation) and digital sampling at a rate of 2000 Hz. It is the authors' experience that preprocessing of the vibration signal greatly improves the quality of the models produced. Envelope detection of the vibration signal (McFadden 1984) was necessary for the detection of faults in this situation. This was because the radial loading of the bearing caused amplitude modulation in the vibration signal. For example, a defect on the inner race will only periodically pass through the loaded zone, thus a variation in strength of the vibration signal will be encountered.

Demodulation was performed by band-passing the vibration signal (3 to 5 kHz) using an analogue filter followed by halfwave rectification. The signal was then low-pass filtered at a frequency of 900 Hz for envelope detection and anti-aliasing prior to sampling. Once digitally sampled, each set of data was normalised in the range from 0.0 to 1.0. This normalisation process was required so that the data remained compatible with the Backpropagation neural networks.

11 RESULTS

The first task involved the construction of the autoregressive models for each class of bearing fault. This was an iterative trial and error procedure for each model. The procedure is as follows (described in further detail by Baillie and Mathew (1994)):

1. Estimation of the model order. This involves the selection of the number of past inputs needed to model the vibration signature accurately. In the case of a double layer neural network, this corresponds to selecting the number of input nodes. The number of number of hidden nodes in the network must also be determined.
2. Estimation of model parameters. Once the structure of the model has been determined, the parameters of the model need to be estimated. For a neural network, it requires training using the Backpropagation algorithm.

Model validation. The performance of the model has to be tested. If the performance of the model is not sufficient, the entire process must be repeated. The optimal Backpropagation models chosen in this investigation for each class of fault are outlined in Table 3. Very accurate models were able to be built for the inner race and the outer race faults. The rolling element fault data was a lot harder to model accurately because the signal was quite noisy. It was extremely difficult to build an accurate model of the normal bearing vibration signal, because the signal was largely random in nature and did not have any strong periodic content.

Table 3. Summary of Optimal Backpropagation Models

Model	Architecture (input/hidden/output nodes)
Inner Race Fault	45/20/1
Outer Race Fault	20/5/1
Rolling Element Fault	20/5/1
No Fault	10/8/1

Once the models for the system had been selected, the next task was to build the classifier. Baye's rule with a number of simplifying assumptions was used. It was assumed that the Signal to Noise ratios emanating from the autoregressive models were Gaussian in distribution, and their means and variances were obtained by testing a number of time series data samples. The a priori probabilities of the occurrence of each class of fault was assumed to be equal (ie, the probability of an inner race fault was assumed to be as equally likely as a normal bearing condition). The Baye's classifier outputs a Probability of Fault Existence for each class of fault.

The performance of the fault diagnostic system was evaluated for the effect of vibration data length from the bearing test rig. Generally, the statistical fluctuations will be better filtered out by long lengths of data. However, long data lengths may not always be available in practice. (In this paper, the data length is defined as the number of successive vectors presented to the model. Thus the true data length would be calculated as the model order and the number of presentations. At the sampling rate of 2000 Hz, one complete revolution of the machine shaft is 40 points. Thus 500 vector presentations approximately represents 13 revolutions of the shaft. Conversely, 25 vectors represent 0.88 revolutions for the no fault model and 1.75 revolutions for the inner race fault model.)

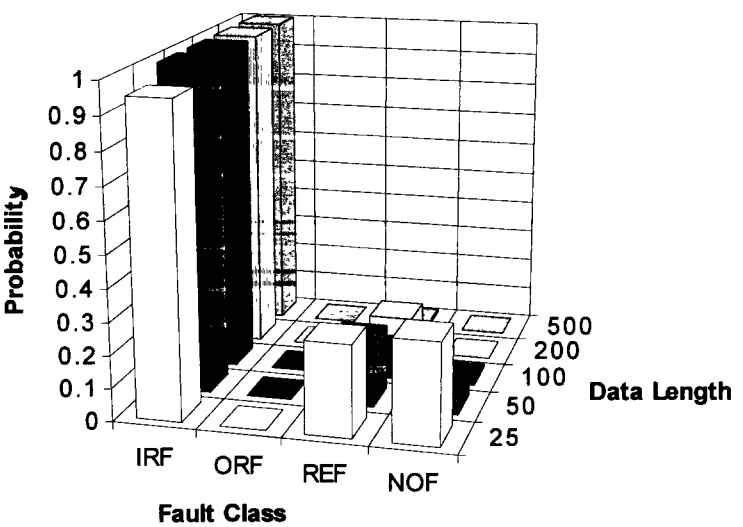

Figure 10. Probability of Fault Existence for an Inner Race Fault of a normal bearing condition indicated by the system, which diminishes with increasing data length.

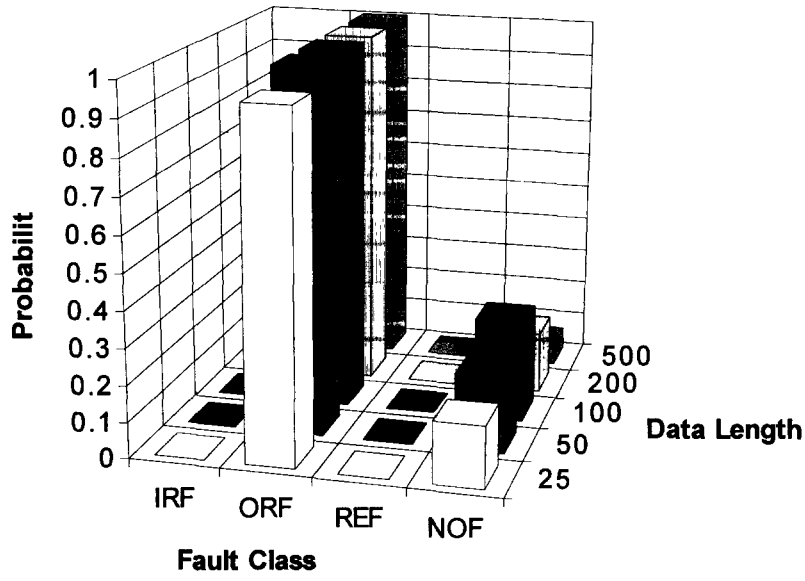

Figure 11. Probability of Fault Existence for an Outer Race Fault

The average performance of the diagnostic system upon the presentation of an inner race fault in the bearing is shown in Figure 10. The probability of fault existence for an inner race fault is close to 1.0, and remains almost independent of the number of vector presentations made to it. For 500 time series vector presentations to the system, the probability of Fault Existence is 1.0 for an inner race fault, and 0.0 for all the other classes of faults. Thus the system is very reliable and robust. At shorter data lengths, the probability of fault existence of an inner race fault remains close to 1.0, however, there is a slightly erroneous indication of a rolling element fault and normal condition. For short data lengths, the performance and reliability of the system is slightly degraded.

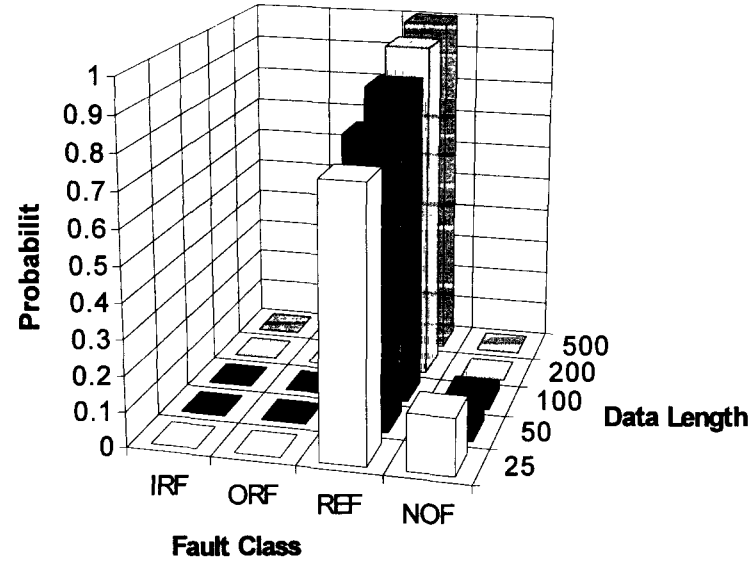

Figure 12. Probability of Fault Existence for a Rolling Element Fault

The presence of an outer race fault can be seen to provoke a strong response from the system (Figure 11). The probability of fault existence is approximately 1.0 for an outer race fault, independent of the number of vector presentations. However, there is also an erroneously small probability for a normal condition.

The presence of a rolling element fault can generally be classified accurately by the system (Figure 12). At very short data lengths the system performance is degraded, as the probability of fault existence for a roller fault is only 0.76 on average, and for a normal bearing it is 0.16 (data length of 25 vectors). However, system performance becomes quite reliable for more than 100 vector presentations.

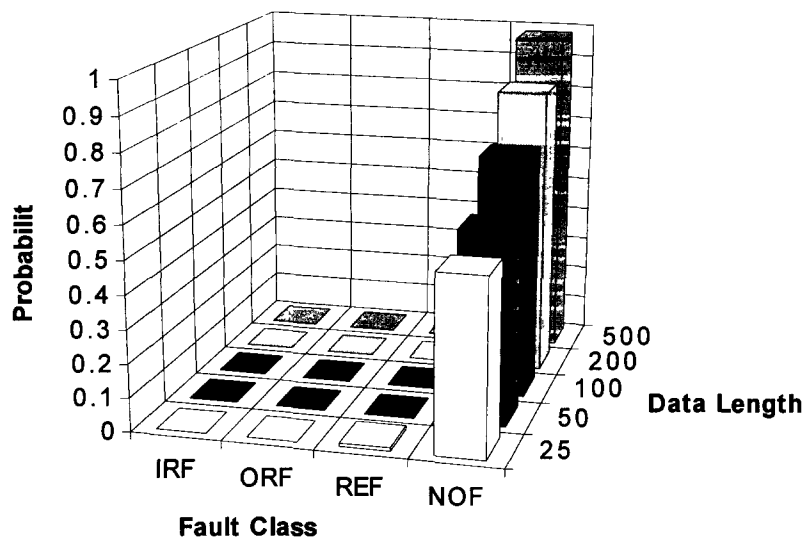

Figure 13. Probability of Fault Existence for a Normal Bearing

The probabilities of fault existence for a typical normal bearing vibration signature is illustrated in Figure 13. In all cases, in terms of data lengths, the vibration signal is classified as pertaining to a normal condition bearing. However, at short data lengths the probability of fault existence is quite low. This is likely to be attributed to the fact that it was difficult to build an accurate model of the normal bearing vibration signal. Longer data lengths help to smooth out the statistical fluctuations.

12 DISCUSSION ON MODEL BASED FAULT DIAGNOSIS

A new approach of directly diagnosing faults from the time domain vibration signal has been investigated in this study. The model-based approach has a number of benefits over methods based on the analysis of the spectrum for rotating machinery fault diagnosis.

The most attractive feature of model-based fault diagnosis is that only short data lengths are required for classification of machine faults. This investigation has shown that as little as 25 time series vector presentations (corresponding to approximately one shaft revolution) can provide accurate and reliable diagnosis of faults in the rolling element bearing. Of course, limitations on the minimum data length are based upon the content of extraneous noise in the signal. Noisy signals mean that accurate models of the fault are difficult to build, and signal lengths for diagnosis need to be longer so that the noise can be averaged out of the signal. Noise can also be eliminated from signals by appropriate data preprocessing techniques.

The fault diagnostic system proposed here is largely modular in concept. Each class of fault is associated with a parametric model. Individual models can be added or removed from the system as required with minimal disruption.
The system is suited to real time classification of faults. This makes it particularity suitable for continuous monitoring of high risk machinery. The availability of microelectronic neural network chips will allow the system to be developed as a stand alone device that might be dedicated to monitoring machinery in remote locations or provide a basis of a portable diagnostic instrument for technicians.
The biggest drawback of the proposed system is the large amount of representative data which must be available prior to training the models. A separate model also has to be specifically built for each type of fault to be identified. For these reasons the system will probably find its niche in the monitoring and diagnosis of simple machine elements, such as rolling element bearings. Conversely, the system maybe applied in a simplistic manner for fault detection. The system might simply consist of one model which would give a "go" or "no go" status.

13 CONCLUSION

Generally condition monitoring is about using a syndrome approach to detect, diagnose and prognose machinery condition. This presentation has been concerned with two of the more recent techniques.

The correlation dimension was shown to be an effective parameter for detecting the existence of a bearing fault and has the potential to differentiate between various bearing faults for diagnostic purposes. The correlation integral is relatively easy to compute, but requires powerful personal computers to reduce computation times. Further work needs to be carried out to determine the suitability of the parameter d_G for practical deterioration trending in comparison with other established techniques.

The time series model-based system for fault diagnosis of rolling element bearings was shown to be accurate and reliable. Nonlinear autoregressive models implemented using backpropagation neural networks was also shown to provide adequate modelling of the vibration data for even very short signal lengths. This technique shows promise in the monitoring of slow speed machinery or bearings running under transient conditions where only limited amounts of data are available.

The bottom line of accurate diagnosis is the need to use all these techniques collectively to highlight different aspects of the time waveform. One would then corroborate the evidence of failure so obtained with results of measurement of condition using other techniques such as wear debris analysis and electrical parameter analysis.

14 REFERENCES

- Baillie, D.C. and Mathew, J. (1994) Nonlinear Model-Based Fault Diagnosis of Bearings, Proceedings of Condition Monitoring '94, Swansea, UK, pp 241 to 252.
- Baker G.L. and Gollub J.P. (1990) Chaotic dynamics - an introduction. Cambridge University Press.
- Box, G.E.P., and Jenkins, G.M., (1976) Time Series Analysis, Forecasting and Control, Revised Edition, Holden Day
- Crutchfield J.P., Farmer J.D., Packard N.H. and Shaw R.S. (1986) Chaos. Scientific American 255, 38-49.

- Froehling H., Crutchfield J.P., Farmer J.D., Packard N.H. and Shaw R. (1981) On determining the dimension of chaotic flows. Physica D 3, 605-617.
- Grassberger P. and Procaccia I. (1983a) Estimation of the Kolmogorov entropy from a chaotic signal. Physical Review A 28, 2591-2593.
- Grassberger P. and Procaccia I. (1983b) Measuring the strangeness of strange attractors. Physica D 9, 189-208.
- Grassberger P. and Procaccia I. (1983c) Characterisation of strange attractors. Physical Review Letters 50, 346-349.
- Greenside H.S., Wolf A., Swift J.B. and Pignataro T. (1982) Impracticality of a box counting algorithm for calculating the dimensionality of strange attractors. Physical Review A 25, 3453-3456.
- Kreysig E. (1988) Advanced Engineering Mathematics. Sixth Edition, John Wiley & Sons, 1285.
- Logan D.B., Plummer D.J. and Mathew J. (1992) A computer implementation of the correlation integral for the calculation of fractal dimension. Centre for Machine Condition Monitoring Research Bulletin, Vol. 4, No. 1.
- Mathew J. (1987) Machine Condition Monitoring using Vibration Analsyses, Acoustics Australia, Vol 15, No 1, pp. 3-13.
- McFadden, P.D. and Smith, J.D. (1984) Vibration Monitoring of Rolling Element Bearings by the High Frequency Resonance Technique - A Review, Tribology International, Vol 17, No 1, pp 3 to 10.
- Möller M., Lange W., Mitscke F., Abraham N.B. and Hübner U. (1989) Errors from digitizing and noise in estimating attractor dimensions. Physics Letters A, 138, 176-182.
- Rumelhart, D. and McClelland, J. (Eds) (1986) Parallel Distributed Processing: Explorations in the Microstructure of Cognition, Vol 1, MIT Press, Cambridge, Massachusetts.
- Simm C.W., Sawley M.L., Skiff F. and Pochelon A. (1987) On the analysis of experimental signals for evidence of deterministic chaos. Helvetica Physica Acta 60, 5410-5457.